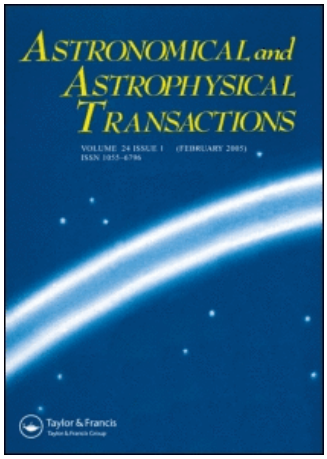

Astronomical & Astrophysical Transactions
The Journal of the Eurasian Astronomical Society
Publication details, including instructions for authors and subscription information:
http://www.informaworld.com/smpp/title~content=t713453505

IPS tomographic observations of 3D solar wind structure

M. Kojima [a]; M. Tokumaru [a]; K. Fujiki [a]; K. Hayashi [b]; B. V. Jackson [c]
[a] Solar-Terrestrial Environment Laboratory, Nagoya University, Nagoya, Aichi, Japan
[b] W.W. Hansen Experimental Physics Laboratory, Stanford University, Stanford, CA, USA
[c] Center for Astrophysics and Space Sciences, University of California, La Jolla, CA, USA

Online Publication Date: 01 December 2007
To cite this Article: Kojima, M., Tokumaru, M., Fujiki, K., Hayashi, K. and Jackson, B. V. (2007) 'IPS tomographic observations of 3D solar wind structure', Astronomical & Astrophysical Transactions, 26:6, 467 - 476
To link to this article: DOI: 10.1080/10556790701596200
URL: http://dx.doi.org/10.1080/10556790701596200

Astronomical and Astrophysical Transactions
Vol. 26, No. 6, December 2007, 467–476

IPS tomographic observations of 3D solar wind structure

M. KOJIMA*†, M. TOKUMARU†, K. FUJIKI†, K. HAYASHI‡ and B.V. JACKSON§

†Solar-Terrestrial Environment Laboratory, Nagoya University,
Furo-cho, Chikusa-ku, Nagoya, Aichi, 464-8601, Japan
‡W.W. Hansen Experimental Physics Laboratory, Stanford University,
455 Via Palou, Stanford, CA 94305-4085, USA
§Center for Astrophysics and Space Sciences, University of California,
San Diego, 9500 Gilman Drive, La Jolla, CA 92093-0424, USA

(Received 19 July 2007)

Interplanetary scintillation (IPS) observations have been improved by development of deconvolution methods for the line-of-sight integration effect. One deconvolution method is to use a computer-assisted tomographic analysis (CAT) technique. In this work, four different kinds of CAT method have been developed. Two of them can be applied to stable solar wind structure in the solar minimum phase, one to quasi-stable solar wind, and the other can derive the three-dimensional structure of transient solar wind events, such as a CME. IPS measurements have enough spatial resolution and accuracy to collaborate with spacecraft observations and theoretical studies of the solar wind. Here, these computer assisted tomographic deconvolution methods are introduced and their application to solar wind studies is described.

Keywords: Interplanetary scintillation; Computer-assisted tomography; Solar wind

1. Introduction

Radio waves from a compact radio source are scattered by electron density irregularities in the solar wind, and the scattered radio waves interfere with each other as they propagate to the Earth, producing diffraction patterns on an observer's plane. This phenomenon is called interplanetary scintillation (IPS). Since Hewish *et al.* [1] developed the IPS technique, it has been used to study the three-dimensional solar wind structure to advantage over some *in situ* spacecraft measurements. It can observe three-dimensional solar wind in a short time, and the observations can be carried out consistently over a solar cycle. However, because of the IPS line-of-sight (LOS) integration effect, solar wind had to be studied with blurred images. The previously used method assumed that IPS observed the solar wind at the so-called P-point, which is the closest point to the Sun of the line of sight. In the late 1990s, new methods of IPS observation and analysis, which can deconvolve the LOS integration effect, were developed independently by a group at the University of California at San Diego [2]

*Corresponding author. Email: kojima@stelab.nagoya-u.ac.jp

Astronomical and Astrophysical Transactions
ISSN 1055-6796 print/ISSN 1476-3540 online © 2007 Taylor & Francis
http://www.tandf.co.uk/journals
DOI: 10.1080/10556790701596200

and another group at the Solar-Terrestrial Environment Laboratory, Nagoya University [3–5]. The method developed by the UCSD group uses remotely separated multi-antennas with a baseline longer than a Fresnel radius, and the other method employs the computer-assisted tomography (CAT) method, which we introduce in this paper.

Four different CAT methods are developed. One is named the corotating tomographic method, which can be used to analyse temporarily stable solar wind structure. The second is the time-sequence tomographic method, which can be used for slowly varying solar wind structure. The third method is MHD-IPS tomography in which MHD simulation is incorporated with IPS observations using a tomographic method. The last one is time-dependent tomography, which can be applied to propagating CME measurements. Time-dependent tomography is not discussed in this paper but is introduced by Jackson *et al.* in another paper in this volume.

2. Corotating tomography

With IPS observations made while the Sun rotates, both the solar rotation and solar wind outward motion give perspective views of three-dimensional solar wind structures at different view angles. These conditions make it possible to use the CAT technique for the IPS analysis. The tomographic analysis is illustrated in figure 1. An initial model of the solar wind velocity distribution is first introduced on a reference sphere and then expanded radially outward with a constant velocity to make a three-dimensional solar wind model. IPS observations are simulated in this solar wind model for the actual observed geometries of lines of sight and then compared with the observed IPS velocity. The discrepancy ΔV between the simulated and

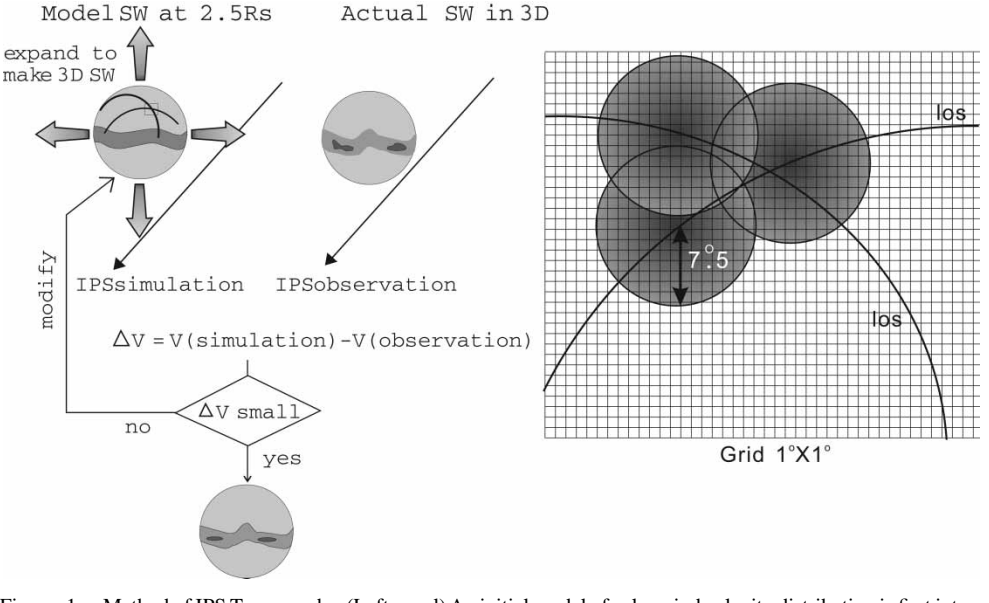

Figure 1. Method of IPS Tomography. (Left panel) An initial model of solar wind velocity distribution is first introduced on a reference sphere and then expanded radially outward with a constant velocity to make a three-dimensional solar wind model. IPS observations are simulated in this solar wind model and then compared with observed IPS velocity. The discrepancy ΔV between the simulated and observed velocities is used to modify the solar wind velocity distribution on the reference sphere. (Right panel) The line of sight is projected on a reference sphere which has a resolution element size of 1 deg $\times$1 deg in longitude and latitude. This line will pass through some of the resolution bins. The discrepancy value of ΔV and a significance factor Ω are assigned to neighbouring bins within angular distance of $\pm$7.5 deg.

observed velocities is distributed on the reference sphere as follows. A line of sight is projected on a reference sphere which has a resolution element size of 1 deg ×1 deg in longitude and latitude. This line passes through some of the resolution bins in the model matrix. For each point along the ray path, a procedure checks if neighbouring bins are within an angular distance of ±7.5 deg. The discrepancy value of ΔV is assigned to those bins with a significance factor Ω. The significance factor Ω consists of the IPS speed estimation error $\sigma_{V_{obs}}$, an angular distance ϕ from the line of sight and a weight factor $\omega(z)$:

$$\Omega = \exp\left(-\frac{3\sigma_{V_{obs}}}{V_{obs}}\right)\exp\left(-\frac{2\phi^2}{7.5^2}\right)\omega(z). \tag{1}$$

The weight function $\omega(z)$ [6] is

$$\omega(z) = 2\pi(\delta N_e(z))^2 \int_0^\infty q\,dq\,\sin^2\left(\frac{q^2\lambda z}{4\pi}\right)\exp\left(-\frac{\theta_0^2 q^2 z^2}{2}\right) q^{-\alpha}. \tag{2}$$

z is a distance along a line of sight from the earth. The $\sin^2$ term is the Fresnel propagation filter, and the exp term is a filtering function due to a finite radio source size θ_0. Density fluctuations are assumed to have a power law spectrum $q^{-\alpha}$. After completing the simulations for all observations, the initial solar wind model is modified with ΔV and Ω, and then the next IPS simulations are restarted. This process is iterated until the residuals become small enough. Usually this process converges after several iterations, giving a result that does not depend on the initial model.

The corotating tomography technique assumes that solar wind structure is temporally stable while the Sun rotates and that the structure at longitude 0° is continuous with that at longitude 360°. Therefore, a line of sight can be projected across the longitudes 0° and 360° as shown in figure 2. If the amount of lines of sight for one solar rotation is not sufficient for the tomographic analysis, data for several rotations have to be combined. In the solar minimum phase, solar surface features show little evolution in consecutive rotations, and we expect that the detrimental effects on the tomography analysis from evolution of solar structures during these periods are small. For a full description of the CAT analysis method, we refer the reader to Asai *et al.* [3] and Kojima *et al.* [4].

Figure 3 demonstrates how the IPS CAT analysis can improve velocity map. The left map is derived from the IPS data obtained during Carrington rotations 1909–1913 (April–September 1996) using the previous P-point assumption, which assumes the IPS observes the solar wind at the closest point to the Sun of the line of sight. Although the analysed period is in the solar minimum phase, velocities at high latitudes are lower than 700 km s^{-1}, and the separation between low-speed and high-speed regions is not distinct. The right map gives the results of the CAT analysis. We see that this map has high resolution and recovered velocities higher than

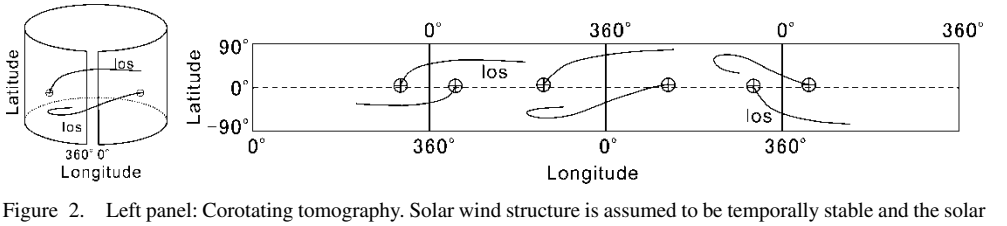

Figure 2. Left panel: Corotating tomography. Solar wind structure is assumed to be temporally stable and the solar wind structure at longitude 0° is continuous to that at longitude 360°, although there are temporal differences. Right panel: Time-sequence tomography. Consecutive rotations construct a seamless large map, and lines of sight can traverse, crossing longitude 0° and 360° into an adjacent map.

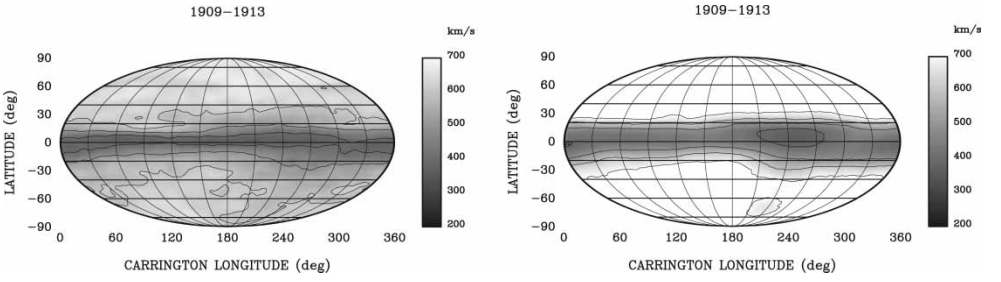

Figure 3. Demonstration of how IPS tomographic analysis improves the velocity distribution map. Left panel is the velocity distribution on the source surface at 2.5 Rs derived with the P-point assumption. Right panel is the result of the tomographic analysis from the same data set used in deriving the left map.

700 km s^{-1} at high latitudes. These features agree well with the solar wind structure obtained by the first Ulysses' rapid latitudinal scan in 1994 and 1995 [7–9].

3. Time-sequence tomography

The corotating tomography cannot be used for the solar maximum phase when the solar wind structure is not stable for a period of a solar rotation. We therefore developed another technique named the time-sequence tomography. In this analysis solar wind structure can change from rotation to rotation if it is quasi-stable for a few weeks. Consecutive rotations construct a seamless, large map as shown in figure 2, and lines of sight can traverse from longitude 0° and 360° into an adjacent map.

Figure 4 shows velocity maps derived with the time-sequence tomography when Ulysses made rapid latitudinal scan in the solar minimum phase (upper panel) and in the solar maximum

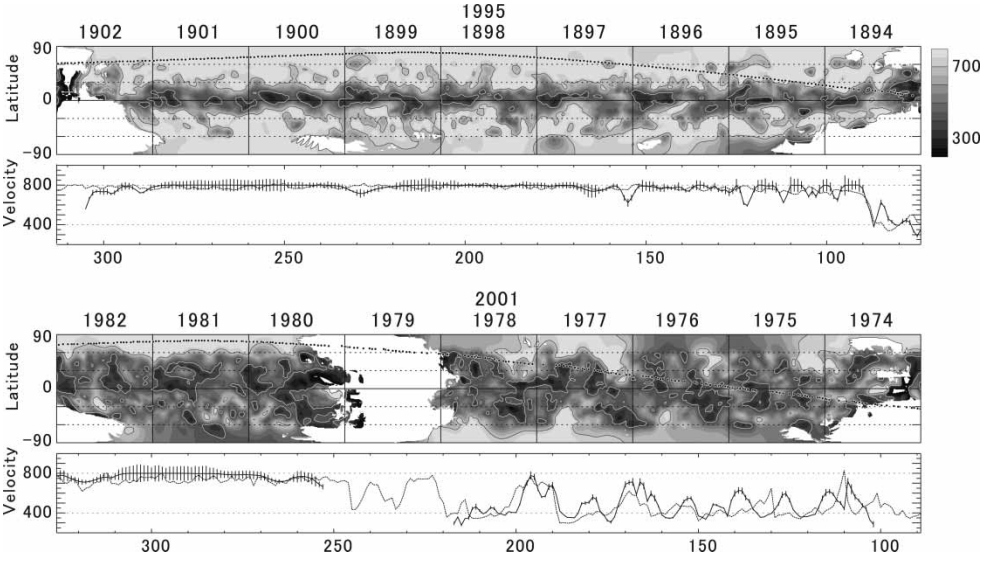

Figure 4. Velocity maps derived from time-sequence tomography when Ulysses made its rapid latitudinal scan at the solar minimum phase (upper panel) and at the solar maximum phase (lower panel). Dots on the maps are Ulysses trajectories mapped back to the reference sphere. Velocities sampled along Ulysses trajectory are plotted with error bars (solid line) in the panel below each map and compared with Ulysses measured velocities (dotted line).

phase (lower panel). Ulysses trajectory is mapped backed onto the maps with a constant radial velocity assumption and shown with dots. Velocities were sampled from the IPS velocity map along Ulysses mapped trajectory and plotted with a solid line in the panel below each map. The Ulysses observations (dotted line) compared with the IPS observations show that the time-sequence tomography can retrieve global solar wind structure even in the solar maximum phase. In these analyses, about 30 lines of sight were obtained per day. If more lines of sight are available, this method allows derivation of less noisy and more reliable velocity maps.

4. MHD-IPS tomography

MHD simulation is a rather common tool used in the study of solar wind dynamics. MHD simulation is derived from initial boundary values. However, actual solar wind structure from the solar surface is more complex than MHD simulations can handle, and at present, there seem to be no models that produce the complex coronal structures well. When the IPS CAT analysis is combined with MHD simulation, CAT analysis can reconstruct an MHD-based three-dimensional solar wind structure, and MHD simulation can obtain observation-based three-dimensional solar wind for a wide range of heliocentric distance and heliographic latitude [10]. Another advantage of MHD-IPS tomography is that it can analyse not only velocity but also other solar wind parameters such as magnetic field, temperature and density. At the same time, an MHD code can simulate the actual conditions in the heliosphere beyond 1 AU by extraporating the results of the MHD tomography analysis.

The MHD tomography analysis is an iterative procedure modifying the solar wind velocity distribution on the inner boundary sphere. The modification of the boundary velocity is made in three steps. In the first step, the MHD simulation of solar wind is carried out using a provisional distribution on the inner boundary at 50 Rs, and the steady state of the three-dimensional MHD-based solar wind is calculated. In the second step, the IPS velocity observations are simulated in this numerical solar wind, and the discrepancies between the velocities from the IPS simulations and the actual IPS observations are calculated for each LOS. In the last step the velocity distribution on the inner boundary surface is modified so that the discrepancies between numerical and actual IPS velocities are reduced. Since the simulation is started from the distance where the solar wind has reached its final cruising velocity, initial boundary conditions of temperature and density can be obtained from the empirical relations with velocity, which are obtained from *in situ* measurements. The magnetic field is derived with a potential field model from photospheric observations, and velocity is determined by MHD-IPS CAT. The MHD simulation can expand solar wind to the outer heliosphere. Solar wind obtained in this way was compared with Ulysses measurements in figure 5. Although the values are not exactly identical in every detail, we note that the major aspects of each solar wind parameter are similar. For a full description of the MHD-IPS tomography, we refer the reader to Hayashi *et al.*[10].

5. Time-dependent tomography

In order to obtain the three-dimensional structure of interplanetary transient phenomena such as a coronal mass ejection event, time-dependent tomography was developed by Jackson *et al.*[11]. In this technique the solar wind is assumed to flow outward following a kinematics model that preserves mass and mass flux, and the changing LOS geometry of the outward flow gives the perspective view of the objects at different view angles. This tomographic technique

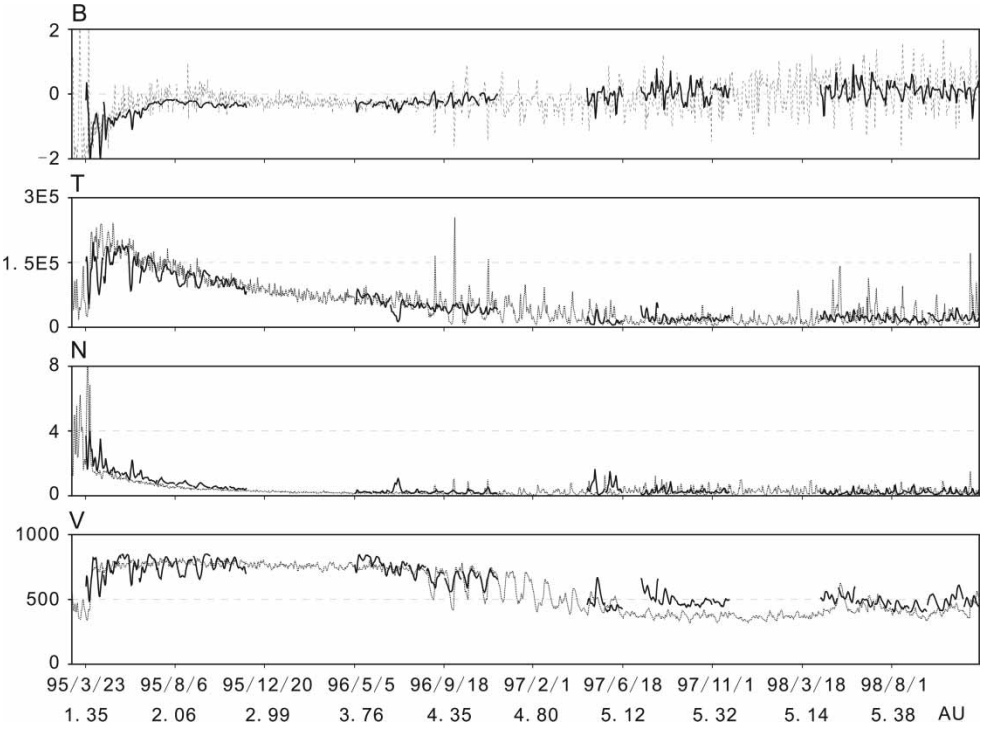

Figure 5. Comparison of MHD-IPS tomography with Ulysses measurements. The solar wind derived from the MHD-IPS tomography is expanded with the MHD code to the Ulysses orbit, and the solar wind parameters obtained from the MHD-IPS tomography (thick solid lines) were compared with Ulysses measurements (thin dotted lines).

can be used to analyse the three-dimensional structure of transient events. A detailed analysis method and application are discussed by Jackson *et al.*in another paper in this volume.

6. Solar wind studies using IPS-CAT

Development of the CAT analysis method has made the interplanetary scintillation method a powerful and useful tool for studying the solar wind. It can retrieve intrinsic solar wind speed with high spatial resolution. With its several advantages over *in situ* measurements, the IPS CAT has been used to study the solar wind. Here we introduce these studies.

6.1 *Latitudinal structure*

Ulysses observed the bimodal velocity structure in the minimum phase and a small but noticeable gradual increase in velocity towards higher latitudes [9]. Velocity asymmetry was also observed in the high-latitude fast wind between the northern and southern hemispheres [8]. Although Ulysses took about ten months to observe these solar wind features at all the latitudes from the south to north poles, the IPS CAT analysis could determine these features in only a few months and confirmed that the N–S asymmetry of the velocity was not caused by temporal change of the solar wind structure during the time Ulysses was taking ten months to make its latitudinal traverse (Figure 6) [12].

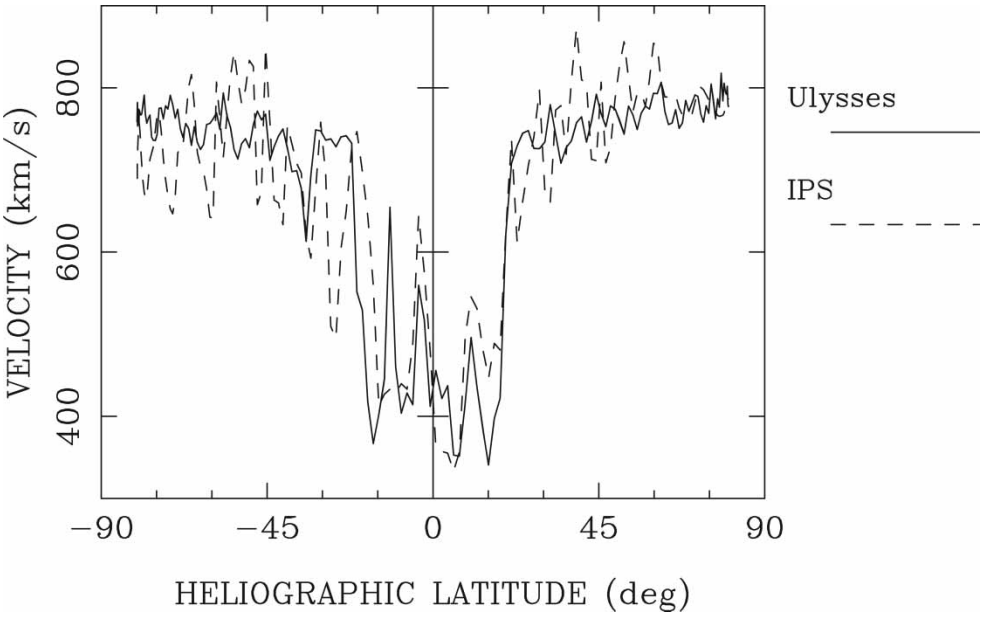

Figure 6. Comparison of latitudinal velocity structures between Ulysses observations (solid line) and IPS CAT analysis (dashed line). A velocity map was derived for the Carrington rotations 1894–1896 from the IPS CAT analysis, and velocities were sampled along the Ulysses trajectory.

6.2 *Origin of low-speed solar wind*

A compact low-speed stream is another object that can test the resolution of the IPS CAT analysis technique. Compact low-speed streams which appeared in the solar minimum phase near the solar equator were studied [13]. One of these (figure 7) is compared on the source surface at 2.5 R_s with coronal potential magnetic field lines. The intersection points of the magnetic field lines with the source surface are labelled by white dots. On the source surface, black areas show velocities $\leq$350 km s^{-1}. In this figure the slowest speed region is not located above the closed loops (helmet structure) but is shifted from them and connected to the open field regions (coronal holes) in the vicinity of the closed loops. Therefore, this compact stream is magnetically unipolar, and consequently a neutral line does not traverse through it. This demonstrates a solution to the long-standing question why the lowest speed locus tends to deviate from a neutral line.

The IPS CAT technique also found another kind of a slow wind source in the polar region at solar maximum when a polar coronal hole became small and was about to disappear in 1990 (CR 1829) and 1999 (CR 1955) [14, 15]. The open fields from the coronal hole were surrounded by closed loops from mid latitudes, forming a large 'sea anemone' type structure. This structure was similar to that of the open field region from a small coronal hole in the vicinity of active regions.

6.3 *Solar wind acceleration mechanism*

Coronal holes play an important role in determining the solar wind structure. A large-scale polar coronal hole is a source of fast solar wind, and medium and slow speed streams originate in smaller coronal holes [16, 17]. Not only the coronal hole scale size but also the flux expansion rate [18, 19] and energy supplied from the photosphere [20] determine the solar wind velocity.

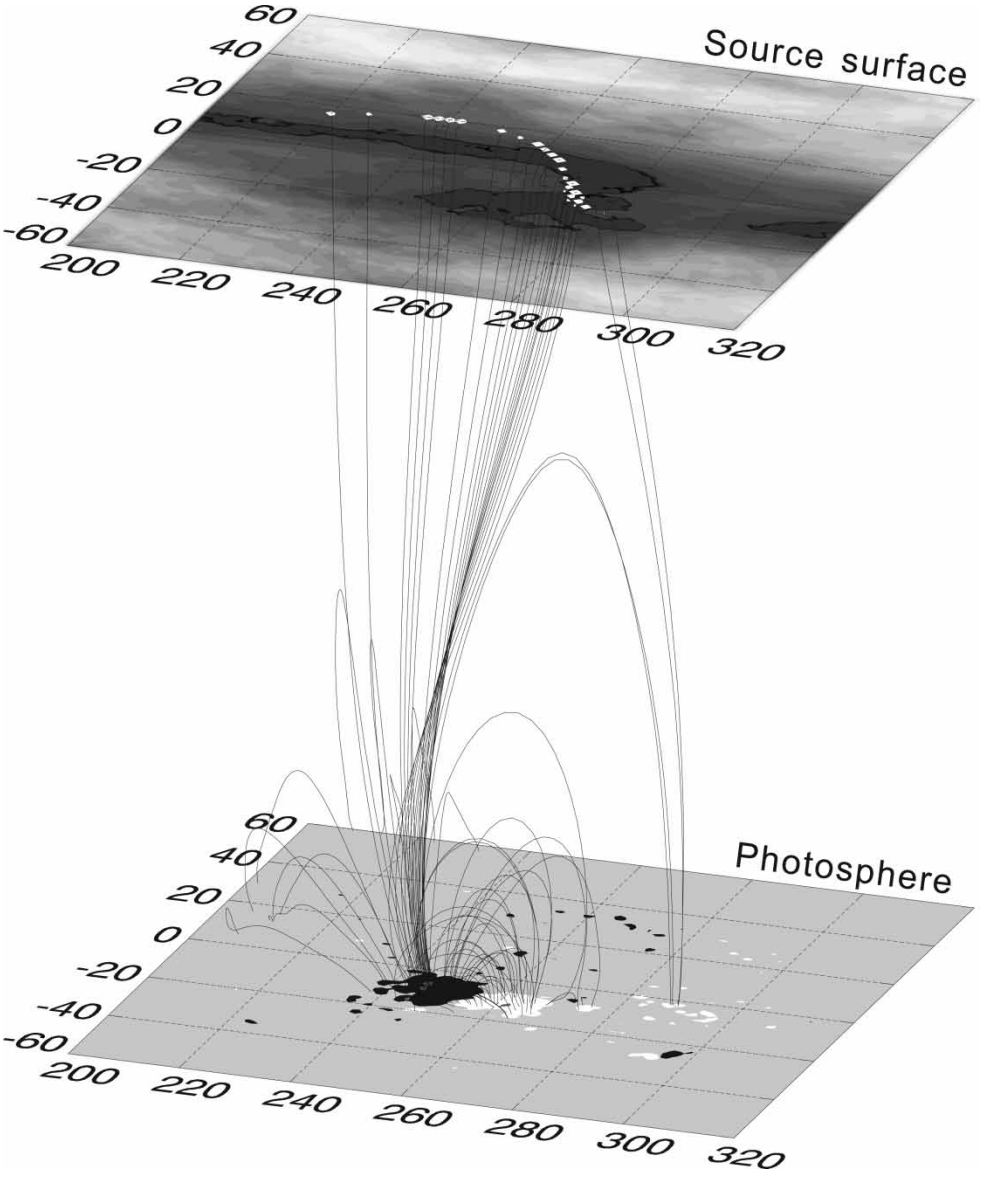

Figure 7. Magnetic potential-field lines shown from the photosphere to the source surface. The longitude and latitude regions are indicated in the figure. Data are for Carrington rotation 1913. Field lines connecting the photosphere and the source surface are shown for an expansion factor >2000, and closed loops in the corona are shown for magnetic field lines stronger than 15 G. Magnetic field lines connected to a polar coronal hole are shown by broken lines. On the source surface, black areas show regions where velocities $<350\,\mathrm{km\,s^{-1}}$, and white spots are locations with a flux-expansion factor ≥ 2000. This figure is adapted from [13].

In order to model the solar wind acceleration it is important to find a universal relation between the global properties of the solar wind and the corona. However, most coronal holes are at high latitudes spacecraft cannot reach, with the exception of the Ulysses. Therefore, the IPS CAT technique, which can derive an unbiased solar wind velocity map over all latitudinal ranges, is an important tool to determine the relation between the wind velocity and the coronal magnetic field conditions. The IPS CAT technique together with coronal magnetic field data

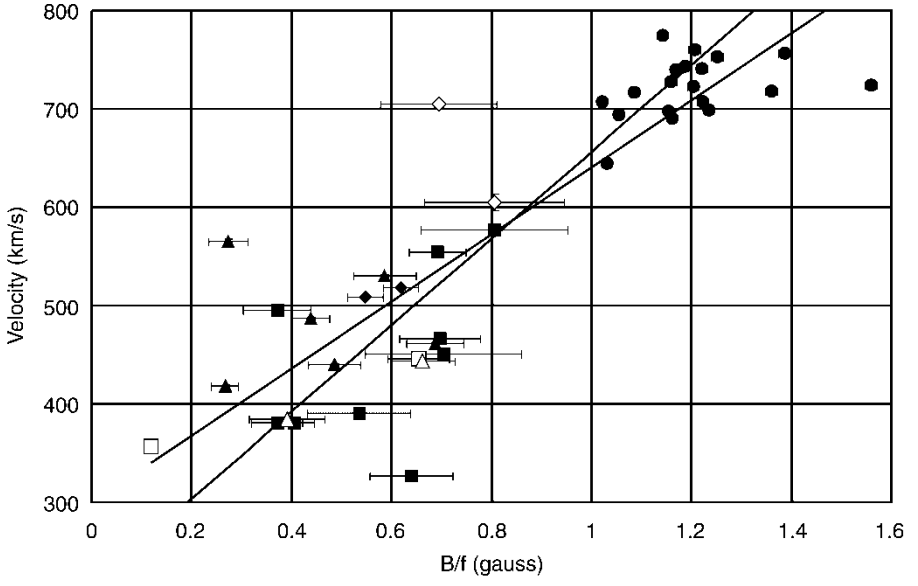

Figure 8. Correlation diagram between velocity and B/f. △ is the equatorial coronal hole associated with active regions with a large flux expansion rate and relatively strong magnetic field, □ is the isolated mid-latitude coronal hole with a medium expansion rate and weaker magnetic field, and ◇ is a polar coronal hole extension with a smaller expansion rate and weaker magnetic field. Two regression lines in the diagram are for V from B/f and for B/f from V, respectively. The correlation coefficient is 0.88. This figure is adapted from [22].

indeed found that a physical parameter combination B/f of the flux expansion rate f, and photospheric magnetic field intensity B has a high correlation with the solar wind velocities from various kinds of coronal holes (figure 8) [21–23].

7. Discussion

The tomographic analysis technique can retrieve intrinsic solar wind speed from LOS integrated IPS measurements and improve spatial resolutions of the IPS measurements. Corotating tomography can derive the detailed solar wind structure in the solar minimum phase from which we can study the latitudinal solar wind structure, origin of low-speed wind and coronal parameters which determine the acceleration mechanism. The time-sequence tomography and the time-dependent tomography can determine solar wind structure from short period observations, and they are now being tested for application to space weather forecasting. MHD-IPS tomography can provide solar wind parameters not only with velocity but also magnetic field, number density and temperature at any heliocentric distance. Thanks to IPS measurements, the solar wind can be observed consistently over a solar cycle and the solar cycle dependence of the solar wind structure has been studied [22].

The IPS at a single frequency cannot observe the solar wind in the full distance range from the Sun to the Earth, and the IPS at a single site cannot monitor the solar wind 24 hours a day. Therefore, international collaboration among IPS facilities operated at different frequencies and different longitudinal sites is very important.

Acknowledgements

We thank Paul Hick of the University of California at San Diego for his collaboration in developing the CAT analysis method. This work was partially supported by the Japan Society for the Promotion of Science (Grants 07454115, 12440130, 15340162, 1634017, 19540473).

References

[1] A. Hewish, P.F. Scott, D. Wills, Nature **203** 1214 (1964).
[2] R.R. Grall, W.A. Coles, M.T. Klinglesmith, A.R. Breen, P.J.S. Williams, J. Markkanen, R. Esser, Nature **379** 429 (1996).
[3] K. Asai, M. Kojima, M. Tokumaru, A. Yokobe, B.V. Jackson, P.L. Hick, P.K. Manoharan, J. Geophys. Res. **103** 1991 (1998).
[4] M. Kojima, M. Tokumaru, H. Watanabe, A. Yokobe, K. Asai, B.V. Jackson, P.L. Hick, J. Geophys. Res. **103** 1981 (1998).
[5] B.V. Jackson, P.L. Hick, M. Kojima, A. Yokobe, J. Geophys. Res. **103** 12049 (1998).
[6] A.T. Young, Astrophys. J. **168** 543 (1971).
[7] J.L. Phillips, S.J. Bame, A. Barnes, B.L. Barraclough, W.C. Feldman, B.E. Goldstein, J.T. Gosling, G.W. Hoogeveen, D.J. McComas, M. Neugebauer, S.T. Suess, Geophys. Res. Lett. **22** 3301 (1995).
[8] B.E. Goldstein, M. Neugebauer, J.L. Phillips, S. Bame, J.T. Gosling, D. McComas, Y.-M. Wang, N.R. Sheeley Jr., S.T. Suess, Astron. Astrophys. **316** 296 (1996).
[9] J. Woch, W.I. Axford, U. Mall, B. Wilken, S. Livi, J. Geiss, G. Gloeckler, R.J. Forsyth, Geophys. Res. Lett. **24** 2885 (1997).
[10] K. Hayashi, M. Kojima, M. Tokumaru, K. Fujiki, J. Geophys. Res. **108** doi:10.1029/2002JA009567 (2003).
[11] B.V. Jackson, P.P. Hick, A. Buffington, M. Kojima, M. Tokumaru, K. Fujiki, T. Ohmi, M. Yamashita, *Proc. 10th International Conference on Solar Wind*, Pisa, Italy, June 17-21, 2002 (AIP Conference Proceedings) **679** 75 (2003).
[12] M. Kojima, K. Fujiki, T. Ohmi, M. Tokumaru, A. Yokobe, K. Hakamada, J. Geophys. Res. **106** 15677 (2001).
[13] M. Kojima, K. Fujiki, T. Ohmi, M. Tokumaru, A. Yokobe, K. Hakamada, J. Geophys. Res. **104** 16993 (1999).
[14] T. Ohmi, M. Kojima, A. Yokobe, M. Tokumaru, K. Fujiki, K. Hakamada, J. Geophys. Res. **106** 24923 (2001).
[15] T. Ohmi, M. Kojima, M. Tokumaru, K. Fujiki, K. Hayashi, K. Hakamada, Geophy. Res. Lett. **30** 1409 (2003).
[16] J.T. Nolte, A.S. Krieger, A.F. Timothy, R.E. Gold, E.C. Roelof, G. Vaiana, A.J. Lazarus, J.D. Sullivan, P.S. McIntosh, Sol. Phys. **46** 303 (1976).
[17] M. Neugebauer, R.J. Forsyth, A.B. Galvin, K.L. Harvey, J.T. Hoeksema, A.J. Lazarus, R.P. Lepping, J.A. Linker, Z. Mikic, J.T. Steiberg, R. von Steiger, Y.-M. Wang, R.F. Wimmer-Schweingruber, J. Geophys. Res. **103** 14587 (1998).
[18] Y.-M. Wang, N.R. Sheeley Jr., Astrophys. J. **355** 726 (1990).
[19] N.R. Sheeley Jr., E.T. Swanson and Y.-M. Wang, J. Geophys. Res. **96** 13861 (1991).
[20] L.A. Fisk, N.A. Schwadron, T.H. Zurbuchen, J. Geophys. Res. **104** 19765 (1999).
[21] M. Hirano, M. Kojima, M. Tokumaru, K. Fujiki, T. Ohmi, M. Yamashita, K. Hakamada, K. Hayashi, Eos Trans. AGU, **84**(46) Fall Meet. Suppl., Abstract SH21B-0164 (2003).
[22] M. Kojima, K. Fujiki, M. Hirano, M. Tokumaru, T. Ohmi, K. Hakamada, Solar wind properties from IPS observations, in *The Sun and the Heliosphere as an Integrated System*, eds G. Poletto and S.T. Suess, Kluwer Academic Publishers, 147 (2004).
[23] M. Kojima, M. Tokumaru, K. Fujiki, H. Itoh, T. Murakami, K. Hakamada, in *New solar physics with solar-B mission, Conference Series of Astronomical Society of the Pacific, The Sixth Solar-B Science Meeting*, Kyoto, 8–11 November 2005, eds K. Shibata, S. Nagata and T. Sakurai, **369** 549 (2007).